Assembled design and compressive performance simulation of mine waterproof wall based on concrete 3D printing

Chuangnan Ren[1,2], Baobin Gao[1,2,3]*, Chenhui Geng[1,2] and Wenjie Zhu[1,2]

[1]State Collaborative Innovation Center of Coal Work Safety and Clean-efficiency Utilization, Jiaozuo, China, [2]School of Safety Science and Engineering, Henan Polytechnic University, Jiaozuo, China, [3]Henan Key Laboratory of Underground Engineering and Disaster Prevention, Jiaozuo, China

With the increase of mining depth, the deep mine waterproof wall project faces the test of worse construction environment and higher risk of water damage. With the development of intelligent construction technology, it is necessary to introduce concrete 3D printing technology for the construction of coal mine waterproof walls, so as to adapt to more complex construction environment and engineering needs. Through uniaxial compression tests, the compressive properties of 3D printed concrete were tested under different printing methods and force directions. The results showed that the compressive strength of the 3D printed concrete was higher under the conditions of printing path B and loading along the direction parallel to the bonding layer. According to test results, the mine waterproof wall structure based on concrete 3D printing was designed. Then, ABAQUS was used to simulate the compressive strength and deformation of the 3D printed waterproof wall. The results showed that the ultimate load of the 3D printing module was $6.697e^4$kN and the deformation range was controllable, which meet the engineering requirements. The advantages of 3D printing mine waterproof walls are more flexible in design, faster in manufacturing, and more intelligent in operation. This work provides new ideas for the design and construction of waterproof walls in deep mines.

KEYWORDS

concrete 3D printing, mine waterproofing wall, assembly design, compressive performance, mining engineering

Introduction

The hydrogeological and engineering geological conditions in deep underground mines have become increasingly complex with continuous increases in the depths of the mines and mining intensity worldwide (Chen et al., 2019; Gao et al., 2021). In China, water inrush disasters are a major threat to the safety of deep underground mines (Sun et al., 2017; Hu and Zhao, 2021; Jiang et al., 2022). Construction of mine waterproofing

walls is one of the most effective and widely applied methods for controlling groundwater and has been used for decades in underground mining (Hang et al., 2022). As the mining depth increases, the construction of mine waterproofing walls is facing the challenge of the worse construction environment and the higher risk of water damage.

Currently, mine waterproofing walls are constructed using the concrete pouring method. When this method is applied to the deep mine engineering site, two technical problems are exposed: on the one hand, the high temperature and high humidity construction environment is likely to cause gaps in the concrete pouring process, which brings hidden dangers to the engineering quality (Kreiger et al., 2019). On the other hand, the traditional construction method involves many sub-projects. It usually takes 2 months to build a waterproof wall, which is difficult to buy time for emergency rescue and disaster relief (Sui and Hang, 2016). In December 2013, the ESW retaining wall system independently developed by a coal mine in Henan Province, China, adopted the method of precast concrete modules to achieve rapid construction in 8 h. This technology subverts the traditional concrete pouring mode, and also provides new ideas for the construction of mine waterproof walls. Since then, the rapid construction of deep mine waterproof walls has become a hot spot in the field. Scholars and engineers have optimized the construction process and put forward new attempts (Gao et al., 2014; Gao and Wang, 2016; Sang, 2016; Gao et al., 2022), which have taken into account the construction conditions of deep mines, but lack green and intelligent measures.

In recent years, intelligent construction technology has achieved rapid development (Bos et al., 2016; Ma and Wang, 2018; Paul et al., 2018; Bai et al., 2021). Compared with prefabricated concrete slabs, 3D printing technology has the advantages of more flexible design, faster manufacturing, and smarter operation (Ma et al., 2018; Wang et al., 2020). In addition, concrete 3D printing can also improve the compression resistance and impermeability of concrete by adding admixtures (such as fibers) (Invernizzi et al., 2016; Rahul et al., 2019). With the development of intelligent construction technology, it is necessary to consider adopting more advanced methods for the construction of coal mine waterproof walls to achieve a faster, greener, safer and more intelligent construction mode.

In view of this, according to the mechanical properties test of 3D printed concrete, a waterproof wall structure based on concrete 3D printing was designed. The compressive performance of the waterproof wall was explored through finite element simulation analysis. Assembled design and compressive performance simulation of mine waterproof wall based on concrete 3D printing provides some new ideas for deep mine disaster prevention and control and the application of concrete 3D printing in mines.

Assembled design of 3D printed mine waterproof wall

Experimental materials

1) Material preparation. The design of 3D printed concrete material composition and mix ratio needs to be coordinated and compatible with the 3D printing system. On the basis of fully considering the properties of raw materials, various mixing principles and preparation methods, determine the proportions of various raw materials, and carry out ingredients according to Table 1.

Among them, the basalt fiber specifications are shown in Table 2. The fiber length is 18mm, which is slightly larger than the 15 mm diameter of the print head, which is beneficial to the orientation effect of the fiber composite material during the extrusion process.

2) Preparation of samples. The HC1008 3D printer was selected for the production of concrete samples. In order to explore the influence of different printing paths on the mechanical properties of concrete, two samples with different printing paths were made to test their mechanical properties. Two 3D printing paths are shown in Figure 1.

The samples were produced using a printing nozzle with a diameter of 15 mm, a printing layer height of 7 mm, and a printing speed of 20 mm/s. Finally, samples of 150 mm×150 mm×150 mm were obtained, as shown in Figure 2.

Experimental setup and method

According to the different stress directions of the samples, it can be divided into two forms: the direction perpendicular to the bonding layer and the direction parallel to the bonding layer. The force perpendicular to the bonding layer is defined as V, and the force parallel to the bonding layer is defined as H, as shown in Figure 3. According to the different printing paths and force directions, four groups (AV, AH, BV, BH) of 12 samples (50mm×50mm×50 mm) were made for uniaxial compression tests to test their compressive performance.

The RMT-150C rock mechanics test system was selected, which adopts the method of applying uniform load vertically on a single axis. The loading rate is 0.005 mm/s, and the vertical load is 1000 kN. The failure phenomenon of the sample is as follows: cracks parallel to the load direction appear on the outer surface of the sample and penetrate the entire sample.
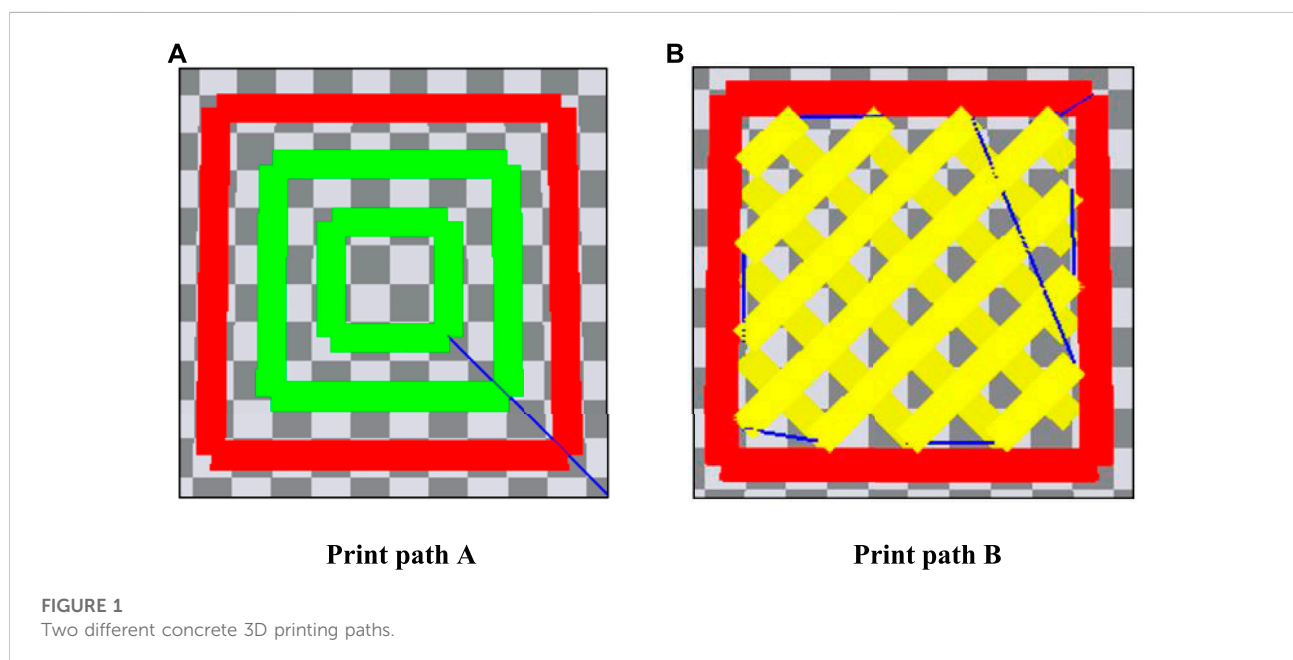
Analysis of results

Under the condition of printing path A, the load-displacement curve of the sample is shown in Figure 4. It shows that under the condition of printing path A, when the

TABLE 1 The ratio of 3D printed concrete materials.

Material	Ordinary portland cement (%)	Silica fume (%)	Basalt fiber (%)	Quartz sand (%)	Water (%)	Set retarder (%)	Water-reducing admixture (%)	Early strength agent (%)
Proportion	100	30	0.5	130	28	0.5	1.2	2

TABLE 2 Specifications of basalt fiber.

Density (g/cm³)	Diameter (um)	Length (mm)	Tensile strength (MPa)	Elastic Modulus (GPa)
2.55	13	18	1950	76.5

Print path A   **Print path B**

FIGURE 1
Two different concrete 3D printing paths.

load is applied perpendicular to the bonding layer, the maximum compressive strength of the sample is 58.511 MPa, and the minimum compressive strength is 51.551 MPa. When the load is applied parallel to the bonding layer, the maximum compressive strength of the sample is 64.179 MPa, and the minimum compressive strength is 60.261 MPa.

Under the condition of printing path B, the load-displacement curve of the specimen is shown in Figure 5. It shows that: under the condition of printing path B, when the load is applied perpendicular to the bonding layer, the maximum compressive strength of the sample is 64.334 MPa, and the minimum compressive strength is 55.211 MPa. When the load is applied parallel to the bonding layer, the maximum compressive strength of the sample is 67.195 MPa, and the minimum compressive strength is 62.393 MPa.

In summary, the overall compressive strength of the samples in the printing path B is higher than that of the samples in the printing path A. This difference is mainly caused by the gap between the adhesive layers. Compared with printing path B, printing path A is more likely to form voids at the corners. Such voids will lead to poorer compactness of the structure, thereby affecting the compressive strength of the structure. Secondly, under the same printing path conditions, the compressive strength of the sample is higher when it is loaded in the direction parallel to the bonding layer. The main reason for this difference is: when loading parallel to the bonding layer, the extension direction of the 3D printing is parallel to the direction of the applied load, and a short column structure is generated inside the concrete, which enhances the compressive strength of the structure. The above experimental results can provide a
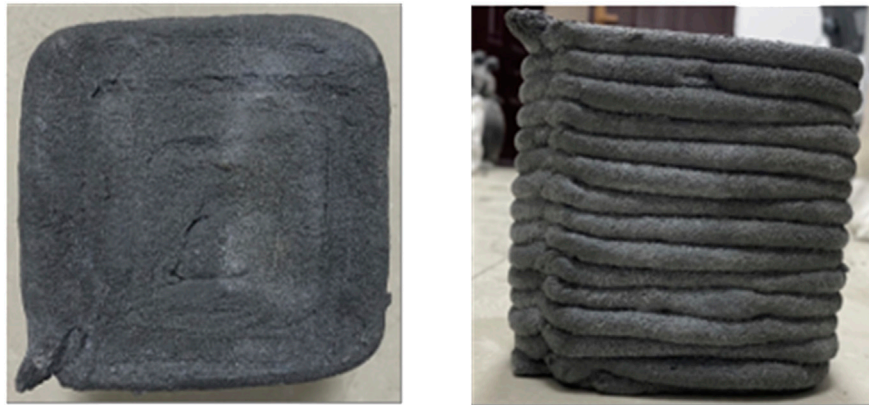
FIGURE 2
3D printed concrete samples.
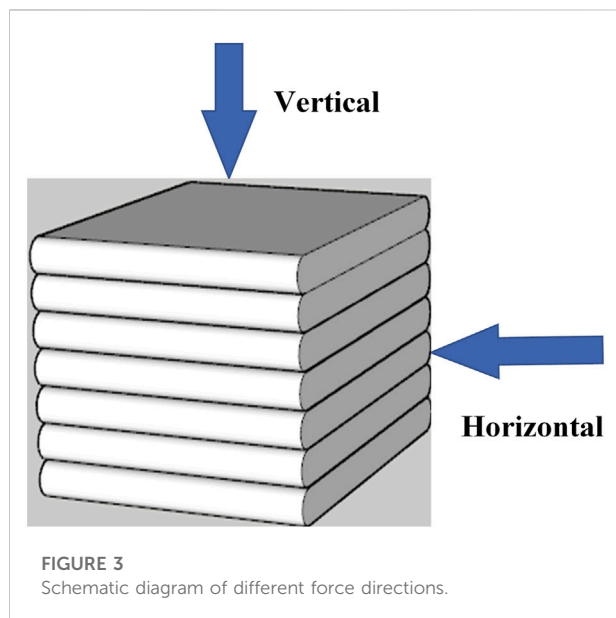
FIGURE 3
Schematic diagram of different force directions.

scientific basis for the design of assembly modules for 3D printed mine waterproof walls.

Assembly module design

The design of the mine waterproof wall is based on a mine in Jiaozuo City, Henan Province, China. The preliminary estimate of the water bearing pressure is 3~5 MPa. According to the design formula in the Chinese coal mine water prevention and control code, the total length of the waterproof wall is 6.6126 m. Considering the actual construction situation and ensuring the safety and stability of the sluice wall, the design

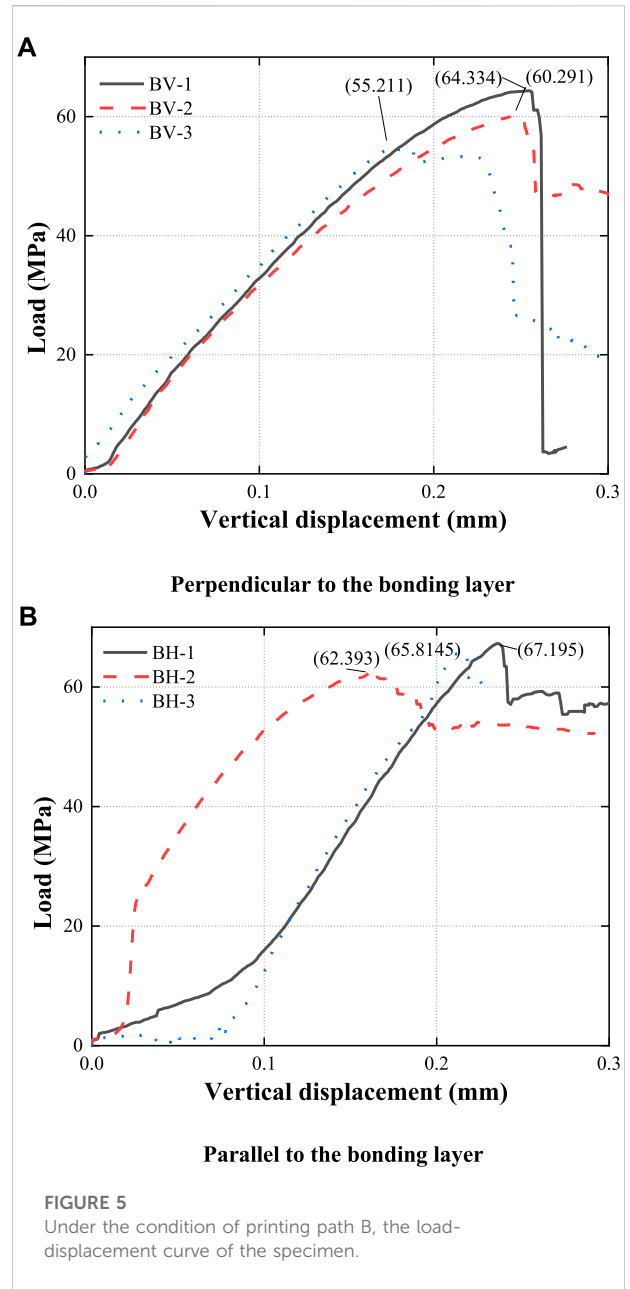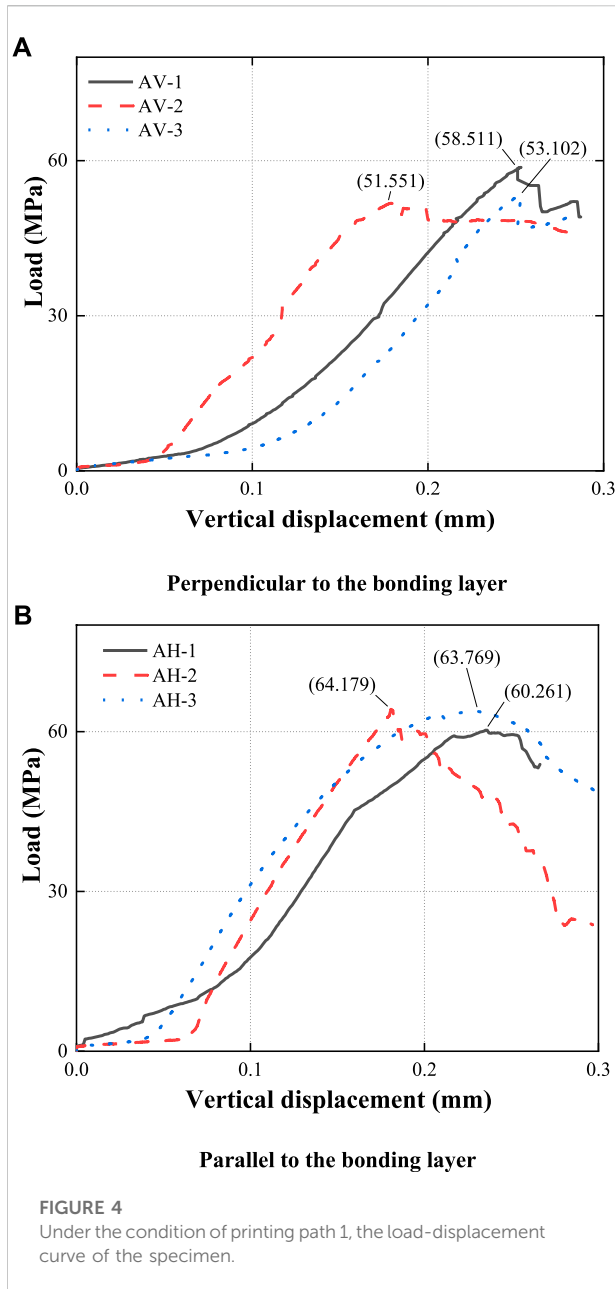values are slightly larger than the calculated values, as shown in Table 3.

The assembly module is 4000 mm long, 4200 mm wide and 1200 mm thick, and the two ends are embedded in the base 300 mm. The protrusions are 400 mm thick and 1000 mm wide. Two bolt holes are preset at 150 mm inward on both sides of the groove, and the diameter of the bolt holes is 20 mm. In order to facilitate the fitting of the module protrusion and the module groove, the gap between the two is 20 mm. Specifically, as shown in Figure 6.

The assembly module adopts the printing path B, and the combined component is subjected to water pressure in the direction parallel to the bonding layer. A total of eight assembly modules are composed, as shown in Figure 7.

Simulation analysis of compressive performance of 3D printed mine waterproof wall

Construction of finite element model

In order to explore the force characteristics of the 3D-printed mine waterproof wall under the action of water pressure and the pressure of the overlying rock, ABAQUS was used for simulation analysis. It was assumed that the upper and lower bases of the main body segment are rigid bodies and will not deform. Only the force transmission and the friction between the surfaces were considered between the assembly modules, and the modules would not have any seepage effect. CDP was adopted as the damage evolution constitutive model of concrete layer material damaged by macroscopic force. For the bonding layer, a Cohesive element was inserted to simulate the interlayer bonding. The concrete strength grade was C30. The meshing element size was

FIGURE 4
Under the condition of printing path 1, the load-displacement curve of the specimen.

FIGURE 5
Under the condition of printing path B, the load-displacement curve of the specimen.

150 mm. As shown in Figure 8, a uniform load of 5 MPa is set in the horizontal direction to simulate the water pressure P. A uniform load of 10 MPa is set in the vertical direction to simulate the overburden pressure F.

Analysis of simulation results

The load-displacement curve of a monitoring point on the stress surface of the structure is shown in Figure 9. It can be seen from the figure that when the load reaches 3.035 e⁴kN and the displacement reaches 0.6mm, the damage starting point is reached. At this time, the curve begins to rise nonlinearly, the stiffness of the structure decreases, and the structure is damaged. When the displacement reaches 2.4mm, the 3D printed structure

TABLE 3 Mine waterproof wall design parameter.

Technical parameter	Calculated	Designed
Chamber length/m	6.61	8
Maximum excavation area/m²	20.83	20.83
Depth of embedded rock/m	0.62	1.5
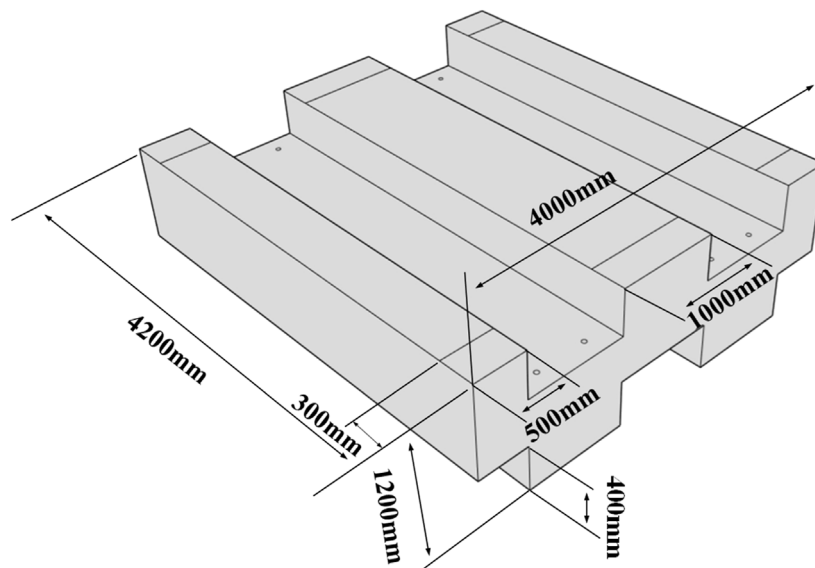
FIGURE 6
Design drawing of 3D printed concrete assembly module.
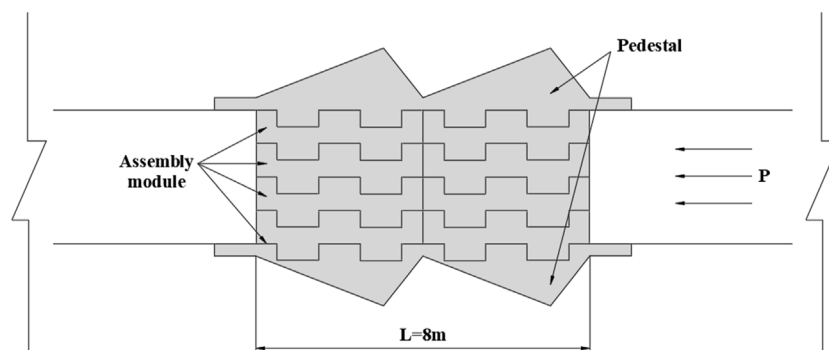
FIGURE 7
Design drawing of 3D printed mine waterproof wall.

reaches the ultimate load 6.697 e^4kN, which is slightly larger than that (6.258 e^4kN) of the conventional structure.

Further, a simulation analysis was carried out for the structural deformation of the 3D printed waterproof wall and the traditional waterproof wall under the action of water pressure. Under the condition of 5 MPa water pressure, when the minimum deformation values are 0.1, 0.05, 0.01, and 0.001mm, the comparison of the deformation ranges of the two models is shown in Figure 10.

According to Figure 10 and the monitored data, the deformation range of the fabricated waterproof wall is slightly larger than that of the traditional one. The deformation range boundary of the traditional waterproof wall is a rounded arc, while the deformation range boundary of the prefabricated waterproof wall is obviously affected by the assembly connection surface. But in general, the deformation range is controllable, which meets the engineering requirements. The advantages of 3D printing mine waterproof walls are more flexible in design, faster in manufacturing, and more intelligent in operation.

Discussions

1) The construction method of 3D printing mine waterproof wall. Based on the above research, a corresponding rapid construction method needs to be formed. At present, the research team has carried out the plan implementation on the project site. The assembly module is pre-printed and formed,
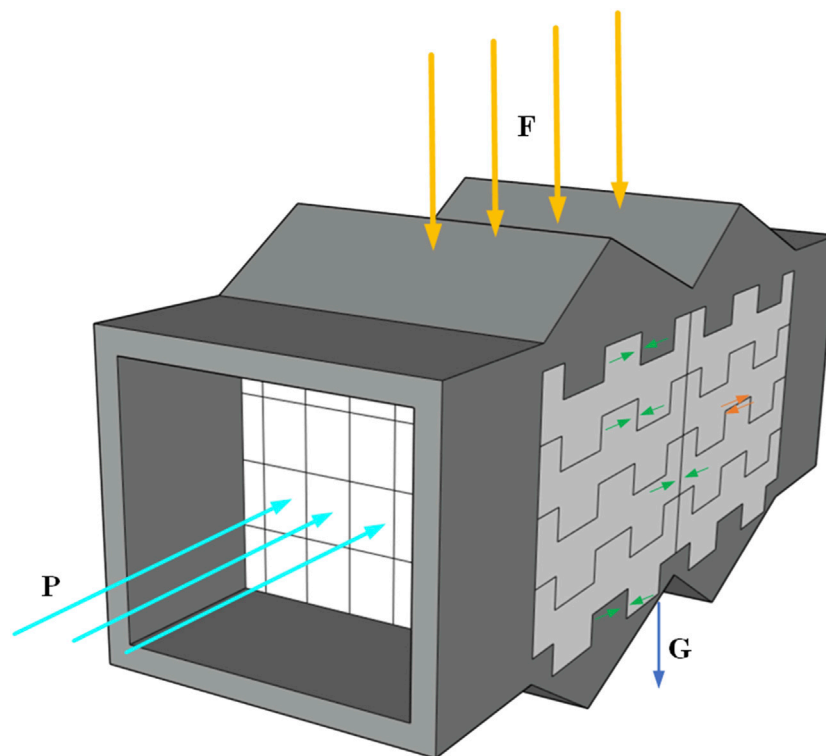
FIGURE 8
Force analysis of 3D printing mine waterproof wall.
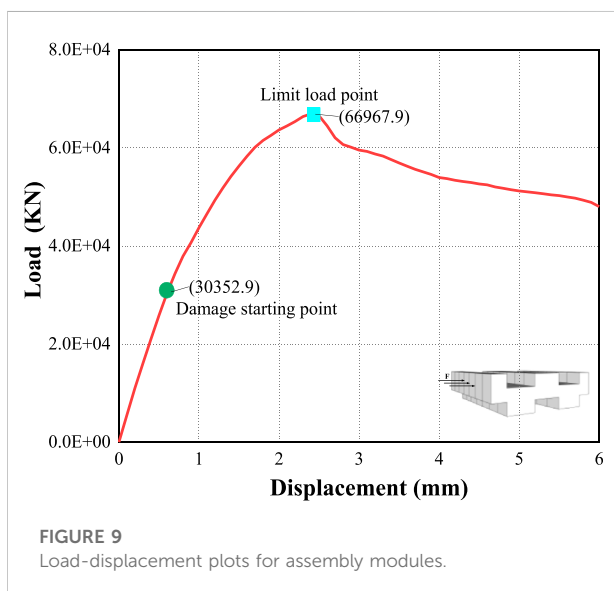
FIGURE 9
Load-displacement plots for assembly modules.

and the rapid assembly of the main section of the sluice wall is completed according to the top-down construction steps. After the assembled modules are assembled, there are a large number of contact seams between the modules, so

the sealing treatment and anti-seepage measures for these gaps are particularly important. The assembly modules are bolted on. The joint work between the modules adopts the hydraulic pressure bonding method of the rubber gasket. The waterproof and anti-seepage performance of the sluice wall structure is ensured by referring to the sealing connection method of the immersed tunnel.

2) Research on the impermeability of 3D printed mine waterproof walls. This work adopted an idealized model, focused on the compressive performance of 3D printed waterproof walls, and believed that the structure has sufficiently strong impermeability. However, as a waterproof structure in mines, it is necessary to conduct further research on the impermeability of 3D printed waterproof walls. The seepage characteristics of 3D printed concrete are different from those of traditional concrete, and the related theory and numerical model need to be improved.

3) Application prospect of 3D printing technology in coal mines. At present, 3D printing technology and prefabricated structures are rarely used in mine construction. With the upgrading and optimization of mine safety technology, it is necessary to consider expanding the application of prefabricated structures to mine engineering. This belongs to the field of interdisciplinary research. 3D printing technology and assembly process help to

FIGURE 10
Comparison of the deformation range of the two models.
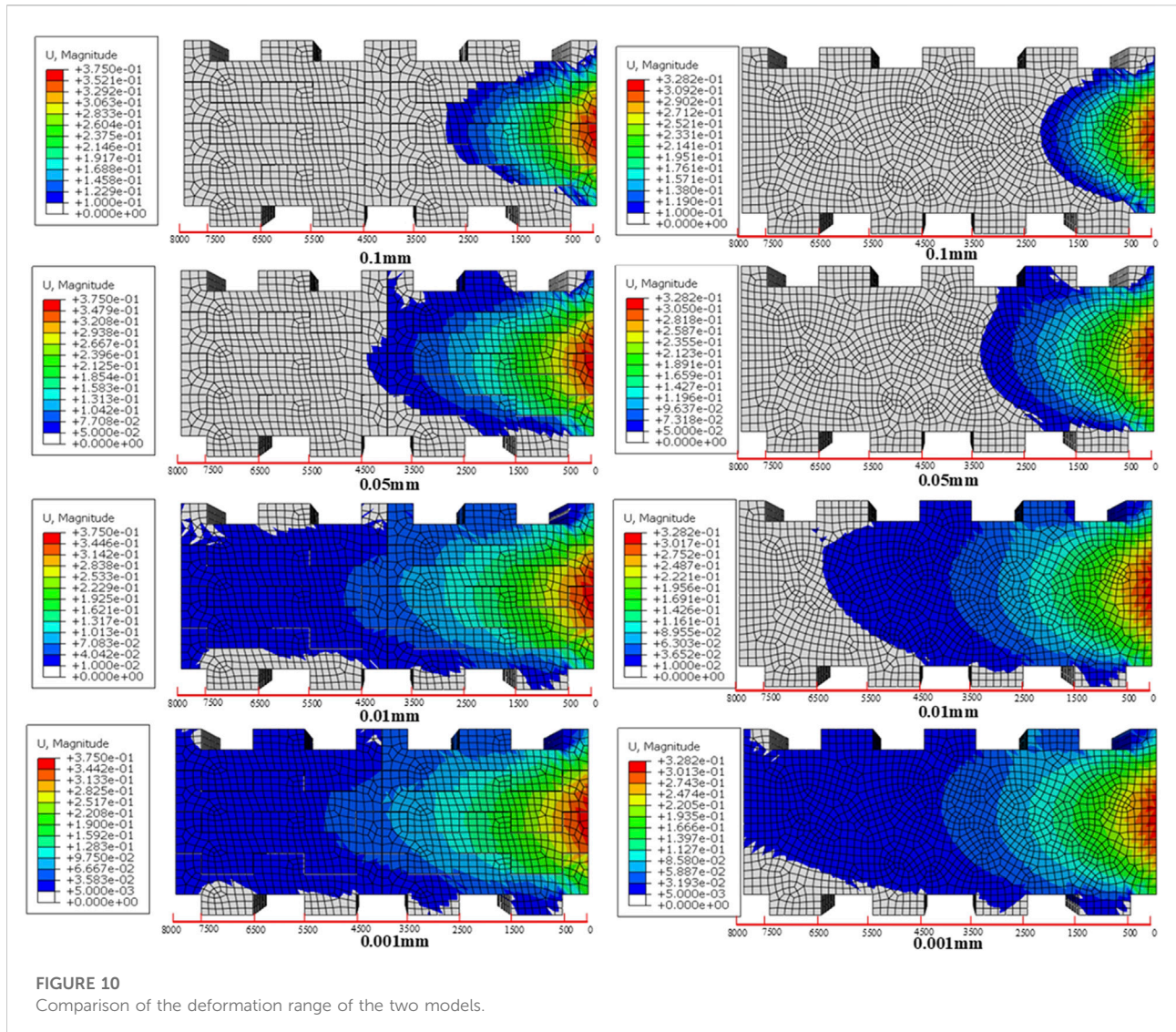
realize the intelligent construction of underground structures in coal mines. Relevant technological innovation and engineering applications need to be strengthened.

Conclusion

1) Four groups of 3D printed concrete were made according to two different printing paths and two force directions. The compressive properties of the 3D printed concrete were tested through uniaxial compression tests. The compressive strength of the 3D printed concrete was higher under the conditions of printing path B and loading along the direction parallel to the bonding layer. According to the test results, a mine waterproof wall structure based on concrete 3D printing was designed.

2) ABAQUS was used to simulate the compressive strength and deformation of the 3D printed waterproof wall. The 3D

printed structure could reach the ultimate load $6.697e^4$kN, which was slightly larger than that ($6.258e^4$kN) of the conventional structure. The deformation range of the 3D printed prefabricated waterproof wall was slightly larger than that of the traditional one. But in general, the deformation range is controllable, which meet the engineering requirements. The advantages of 3D printing mine waterproof walls are more flexible in design, faster in manufacturing, and more intelligent in operation.

3) The construction technology of 3D printing mine waterproof wall was discussed. The water pressure crimping method using rubber gaskets was envisaged to ensure the waterproof and impermeable performance of the waterproof wall structure. As a waterproof structure in mines, it is necessary to conduct further research on the impermeability of 3D printed waterproof walls. With the upgrading and optimization of mine safety technology, it is necessary to consider expanding the application of prefabricated structures to mine engineering.

Data availability statement

The original contributions presented in the study are included in the article/Supplementary Material, further inquiries can be directed to the corresponding author.

Author contributions

CR was responsible for the writing of the article and the construction of the framework; BG initially proposed the innovation of this article and provided great help for the optimization of the article; CG assisted in completing the simulation part and participated in the editing of the article; WZ assisted in completing the experimental part.

Funding

Acknowledgments

Conflict of interest

The authors declare that the research was conducted in the absence of any commercial or financial relationships that could be construed as a potential conflict of interest.

Publisher's note

All claims expressed in this article are solely those of the authors and do not necessarily represent those of their affiliated organizations, or those of the publisher, the editors and the reviewers. Any product that may be evaluated in this article, or claim that may be made by its manufacturer, is not guaranteed or endorsed by the publisher.

References

Bai, X. D., Cheng, W. C., and Li, G. (2021). A comparative study of different machine learning algorithms in predicting EPB shield behaviour: A case study at the xi'an metro, China. *Acta Geotech.* 16 (12), 4061–4080. doi:10.1007/s11440-021-01383-7

Bos, F., Wolfs, R., Ahmed, Z., and Salet, T. (2016). Additive manufacturing of concrete in construction: Potentials and challenges of 3D concrete printing. *Virtual Phys. Prototyp.* 11 (3), 209–225. doi:10.1080/17452759.2016.1209867

Chen, X. J., Li, L. Y., Wang, L., and Qi, L. L. (2019). The current situation and prevention and control countermeasures for typical dynamic disasters in kilometer-deep mines in China. *Saf. Sci.* 115, 229–236. doi:10.1016/j.ssci.2019.02.010

Gao, B. B., Ren, C. N., Dong, Q., and Chen, L. W. (2021). Study on dynamic behavior law and microseismic monitoring in stoping process of roadway with high Gas and wide coal pillar. *Shock Vib.* 2021, 1–14. doi:10.1155/2021/5135964

Gao, B. B., Ren, C. N., and Song, S. P. (2022). A new evaluation method for water blocking performance of coal seam floor: Model construction, case application, and water-preserved strategy. *GEOFLUIDS* 2022, 1–13. doi:10.1155/2022/1608734

Gao, S. X., Wu, S. L., and Ma, H. Y. (2014). Numerical simulation of high-pressure floodgate wall based on FLAC3D. *Saf. Coal Mines* 45 (7), 166–168. doi:10.13347/j.cnki.mkaq.2014.07.050

Gao, Y., and Wang, J. M. (2016). Experiments on instant and automatic construction of movable floodgate wall in mines. *Res. Explor. Laboratory* 35 (3), 60–64.

Hang, Y., Sui, W. H., and Yuan, S. C. (2022). Experimental investigation of the seepage failure between bulkheads and surrounding rocks in deep underground mines. *Bull. Eng. Geol. Environ.* 81 (9), 362. doi:10.1007/s10064-022-02859-w

Hu, W. Y., and Zhao, C. H. (2021). Evolution of water hazard control technology in China's coal mines. *Mine Water Environ.* 40 (2), 334–344. doi:10.1007/s10230-020-00744-0

Invernizzi, M., Natale, G., Levi, M., Turri, S., and Griffini, G. (2016). UV-assisted 3D printing of glass and carbon fiber-reinforced dual-cure polymer composites. *Materials* 9 (7), 583. doi:10.3390/ma9070583

Jiang, H., Fan, G. W., Zhang, D. S., Zhang, S. Z., and Fan, Y. B. (2022). Evaluation of eco-environmental quality for the coal-mining region using multi-source data. *Sci. Rep.* 12 (1), 6623. doi:10.1038/s41598-022-09795-5

Kreiger, E. L., Kreiger, M. A., and Case, M. P. (2019). Development of the construction processes for reinforced additively constructed concrete. *Addit. Manuf.* 28, 39–49. doi:10.1016/j.addma.2019.02.015

Ma, G., Li, Z., and Wang, L. (2018). Printable properties of cementitious material containing copper tailings for extrusion based 3D printing. *Constr. Build. Mat.* 162, 613–627. doi:10.1016/j.conbuildmat.2017.12.051

Ma, G., and Wang, L. (2018). A critical review of preparation design and workability measurement of concrete material for largescale 3D printing. *Front. Struct. Civ. Eng.* 12 (3), 382–400. doi:10.1007/s11709-017-0430-x

Paul, S. C., van Zijl, G. P., Tan, M. J., and Gibson, I. (2018). A review of 3D concrete printing systems and materials properties: Current status and future research prospects. *Rapid Prototyp. J.* 24 (4), 784–798. doi:10.1108/RPJ-09-2016-0154

Rahul, A. V., Santhanam, M., Meena, H., and Ghani, Z. (2019). Mechanical characterization of 3D printable concrete. *Constr. Build. Mater.* 227, 116710. doi:10.1016/j.conbuildmat.2019.116710

Sang, Z. H. (2016). Fast construction technology of water gate wall under flowing water condition. *Coal Chem. Industry* 39 (12), 9–16. doi:10.19286/j.cnki.cci.2016.12.003

Sui, W. H., and Hang, Y. (2016). Review and prospect on design and construction technology of mine water bulkhead. *Coal Sci. Technol.* 44 (8), 7–13. doi:10.13199/j.cnki.cst.2016.08.002

Sun, W., Zhang, S., Guo, W., and Liu, W. (2017). Physical simulation of high-pressure water inrush through the floor of a deep mine. *Mine Water Environ.* 36 (4), 542–549. doi:10.1007/s10230-017-0443-7

Wang, L., Tian, Z., Ma, G., and Zhang, M. (2020). Interlayer bonding improvement of 3D printed concrete with polymer modified mortar: Experiments and molecular dynamics studies. *Cem. Concr. Compos.* 110, 103571. doi:10.1016/j.cemconcomp.2020.103571